J. exp. Biol. **165**, 1–19 (1992)
Printed in Great Britain © *The Company of Biologists Limited 1992*

THE PROFILE DRAG OF A HAWK'S WING, MEASURED BY WAKE SAMPLING IN A WIND TUNNEL

BY C. J. PENNYCUICK[1,*], CARLTON E HEINE[2], SEAN J. KIRKPATRICK[1] AND MARK R. FULLER[3,†]

[1]*Department of Biology, University of Miami, PO Box 249118, Coral Gables, FL 33124-0421, USA*, [2]*Department of Zoology, Duke University, Durham, NC 27706, USA*, and [3]*US Fish and Wildlife Service, Patuxent Wildlife Research Center, Laurel, MD 20708, USA*

Accepted 20 December 1991

Summary

The distribution of dynamic pressure behind a Harris' hawk's wing was sampled using a wake rake consisting of 15 pitot tubes and one static tube. The hawk was holding on to a perch, but at an air speed and gliding angle at which it was capable of gliding. The perch was instrumented, so that the lift developed by the wing was known and the lift coefficient could be calculated. The mean of 92 estimates of profile drag coefficient was 0.0207, with standard deviation 0.0079. Lift coefficients ranged from 0.51 to 1.08. Reynolds numbers were nearly all in the range 143 000–194 000. The estimates of profile drag coefficient were reconcilable with previous estimates of the wing profile drag of the same bird, obtained by the subtractive method, and also with values predicted by the 'Airfoil-ii' program for designing aerofoils, based on a digitized wing profile from the ulnar region of the wing. The thickness of the wake suggested that the boundary layer was mostly or fully turbulent in most observations and separated in some, possibly as an active means of creating drag for control purposes. It appears that the bird could momentarily either increase or decrease the profile drag of specific parts of the wing, by active changes of shape, and it appeared to use the carpo-metacarpal region especially for such control movements. Further investigation in a low-turbulence wind tunnel would help to resolve doubts about the possible influence of airstream turbulence on the behaviour of the boundary layer.

Introduction

Components of drag

The profile drag of the wings is one of three major components that make up the

* Present address: Department of Zoology, University of Bristol, Woodland Road, Bristol BS8 1UG, England.
† To whom reprint requests should be addressed.

Key words: bird, wing, drag, wind tunnel, *Parabuteo unicinctus*.

total drag of a gliding bird, the other two being the drag associated with supporting the weight in air (induced drag) and the drag of the body (parasite drag). For calculations of gliding performance, these three components of drag have to be calculated separately and added together. There is a good theoretical basis for calculating induced drag, as studies of vortex wakes (Spedding, 1987) indicate that the mechanics of supporting the weight are basically the same in gliding birds as in fixed-wing aircraft. Classical engineering methods can be expected to give realistic estimates for this component of drag. Calculation of the parasite drag is usually based on measurements of the drag of wingless bird bodies, such as those by Pennycuick *et al.* (1988) and Tucker (1990*a*,*b*). Profile drag is calculated from the formula:

$$D_{\mathrm{pro}} = 0.5\rho V^2 S C_{\mathrm{Dpro}}\,, \tag{1}$$

where ρ is the air density, V is the air speed and S is the projected area of the wings. The dimensionless number C_{Dpro}, the profile drag coefficient, is in general a function of the lift coefficient. In aeronautical studies on wings with thin, cambered profiles like those of birds, the profile drag coefficient varies most strongly at high lift coefficients, corresponding to low-speed flight. For purposes of performance prediction, it is often assumed to be constant at medium and high air speeds. When comparing flight at different scales, it is also a function of the Reynolds number (Re), defined as:

$$Re = Vc/\nu, \tag{2}$$

where c is the wing chord. Some ornithologists use the term 'chord' in a sense different from its aeronautical meaning, which refers to the distance from the leading to the trailing edge of the wing, along the direction of the airflow (even if the flow is not parallel to the bird's body axis). The chord varies from point to point along the wing. ν is the kinematic viscosity of the air, that is the ratio of the viscosity to the density.

The profile drag coefficient of a bird's wings has never been measured directly in a live bird, although indirect estimates have been made by subtraction. The total drag of a gliding pigeon was determined by Pennycuick (1968), by finding the flattest angle at which the bird could maintain a steady glide in a tilting wind tunnel. Then, calculated values of the induced and parasite drag were subtracted from the total drag to yield the profile drag. The same method was used by Tucker and Parrott (1970) to show that a gliding falcon progressively reduced its wing span with increasing speed, in such a way as to minimize the sum of induced and profile drag. Recently, Tucker and Heine (1990) used this method to investigate the gliding performance of a Harris' hawk in greater detail, and obtained a 'polar plot', that is a diagram relating the profile drag coefficient to the lift coefficient. The lift coefficient was varied by training the bird to glide at a range of different speeds, and the profile drag was obtained as before, by subtracting the induced and parasite drag from the total drag. In the present study we observed the same Harris' hawk, in the same wind tunnel, but measured the profile drag directly.

Nature of profile drag

A wing's profile drag is that part of its total drag which is *not* associated with the creation of a vortex wake. As conventionally defined, profile drag is actually the sum of two components, pressure drag and skin friction drag, which are due to different physical processes and vary in different ways with the air speed. The pressure drag is the difference between the downstream force, due to the integrated static pressure on all forward-facing parts of the surface, and the upstream force, due to the integrated pressure on rearward-facing surfaces. These forces act everywhere normal to the surface. Skin friction drag is due to shear between the layers of air sliding over the surface, and represents forces that are everywhere tangential to the surface. Other things being equal, pressure drag varies with the square of the speed, whereas skin friction drag varies directly with the speed. If pressure drag is the predominant component of profile drag, as is the case on large scales such as those of aircraft wings, it is a good approximation to regard the profile drag coefficient (equation 1) as being independent of speed. However, on the scale of small insects, skin friction drag may be appreciable or even predominant, and in that case the profile drag coefficient, as defined in equation 1, would vary inversely with the speed. These variations of scale are characterised by the Reynolds number as defined in equation 2. At Reynolds numbers typical of birds (10^4–10^6), it is difficult to be sure whether it is satisfactory to assume that the profile drag coefficient will be independent of speed. Explanations of these effects, as they apply to animal wings, may be found in Vogel (1981) and Pennycuick (1989), and a more technical account for engineers is given by Anderson (1984).

Principle of the wake sampling method

In free flight, the profile drag force tends to accelerate the wing in the direction of the relative air flow, but if the wing is held fixed, the reaction decelerates the air flowing past it instead. The magnitude of the drag force can be determined by measuring the amount by which the air flow is slowed down by the presence of the wing. It is possible to find the profile drag by measuring the pressure in an array of pitot tubes, placed behind the wing and pointing into the relative air flow. Profile drag may be represented as the drag due to loss of momentum by the air, in the direction parallel to the flow, whereas induced drag is caused by imparting momentum to the air, in a direction transverse to the flow. Ideally, a pitot tube array would detect only the streamwise variations of air velocity and would not be affected by transverse variations. In practice, drag measurements of this type are not considered reliable where transverse components of flow are strong, for instance near the tip of a wing that is developing lift. They also have to be interpreted with caution if the array intercepts the 'dead' space behind a bluff body or stalled wing, where the boundary layer has separated from the surface. Subject to these reservations, the method measures profile drag only and yields an estimate for the local profile drag coefficient at a particular spanwise position on

the wing. It is not possible to distinguish pressure drag from skin friction drag by sampling pressures in the wake, as in this study, although this can be done on an aircraft wing, by installing a probe very close to the surface.

Materials and methods

Bird and wind tunnel

The bird used in our experiments was a male Harris' hawk (*Parabuteo unicinctus* Temminck). At the time of our observations (11–14 December 1990), the hawk was aged 19 months and had recently completed his moult, so that his plumage was in near-perfect condition. He had previously been trained to fly in the tilting wind tunnel at Duke University, North Carolina, as reported by Tucker and Heine (1990). His mass varied during the experiments from 774 to 836 g. His wing span was 1.03 m and his wing area was $0.186\,m^2$, as measured by the methods of Pennycuick (1989). The wind tunnel was an open-circuit design with an enclosed, rectangular working section 1.38 m wide by 1.08 m high, and a downstream fan. The whole machine could be tilted to permit the bird to glide. Further details of the wind tunnel were given by Tucker and Parrott (1970). The generous size of the working section meant that corrections for tunnel wall interference could be neglected. Estimates from formulae given by Pankhurst and Holder (1965) indicated that the solid blockage and wake blockage factors would be about 2.9×10^{-4} and 1.7×10^{-3} respectively.

Positioning the bird

To obtain an observation with the wake sampling device (below), the bird had to be positioned with his wing just ahead of the pitot-tube array. In preliminary experiments, we tilted the tunnel 4° from horizontal so that the bird could glide, in the hope of obtaining observations in free gliding flight. In the course of trying to train the bird to fly in the right place, we observed that, if allowed to hold on to a perch with one or both feet, he would keep his wings in the flying position, and could be manoeuvred into position as required. We then installed a small perch on a two-component strain gauge balance (also used for calibration tests, below). The lift force measured by the balance, added to the bird's weight, supplied an estimate of the lift developed by the wings. By photographing the bird from below, we were able to estimate his wing area for each individual observation and hence the lift coefficient. There was usually a net upward force on the perch of about 10–50 % of the bird's weight. No special inducement was needed to get the bird to spread his wings and support his weight. He would do this whenever we placed him on the perch in a wind, sometimes for several minutes at a time.

Wing measurements

Each observation of profile drag was initiated by the observer remotely triggering a Pentax SF1 35 mm camera, which was placed on its back on the floor of

the wind tunnel. The camera took a photograph, imprinted with the date and time, of the bird's wing from directly below, also including the tip of the static probe. The local wing chord, immediately upstream of the probe, was measured with Vernier calipers on contact prints of the films, to a precision better than 1 %. The apparent chord on the photographs was scaled by reference to a photograph of a ruler, supported at the position occupied by the bird's wing during observations. The maximum value for the wing length (shoulder to wing tip), seen in frames in which the wing appeared to be fully spread, was assumed to correspond to a wing area of $0.186\,m^2$, as measured from a wing tracing by the method of Pennycuick (1989). In most frames, the wing length was less than the maximum, because of flexion of the elbow and wrist joints, and the area was assumed to be reduced in direct proportion to the wing length (implying constant mean chord). The precision of the area measurements was estimated to be about 5 %, and this would be the predominant source of error in estimating the lift coefficient.

Wake rake

We sampled the wake by means of a 'wake rake' (Fig. 1). This consisted of an array of 15 pitot tubes made of stainless-steel hypodermic tubing of 1.1 mm outside diameter, with the centres spaced 2.2 mm apart, giving a sampling line which measured 30.8 mm from top to bottom. The pitot tubes projected 21 mm into the wind from the upwind face of a hollow, rectangular 8 mm×4 mm brass support stem, which also supported a static pressure probe, 120 mm below the centre pitot tube. The static probe projected 80 mm upwind of the support stem, was 3.2 mm in outside diameter, with a rounded, closed tip, and had four holes equally spaced around the circumference, 28 mm downstream of the tip. The middle pitot tube was 800 mm above the floor of the tunnel (280 mm below the top), and the perch was positioned so that the pitot tube array intercepted the wing wake when the bird spread his wings. The support stem for the pitot tube array was itself fixed to the movable arm of an electrical actuator device (Spectravideo Quickshot SVI-2000A), which was clamped to the floor of the tunnel and could be rotated forward or back remotely. The pitot tubes should ideally be aligned with the local flow behind the wing, which is deflected downwards by the downwash due to the wing. It was not practicable to adjust the orientation of the array for each observation, but calculation indicated that the downwash angle behind the wing should be about the same as the angle at which the tunnel was tilted. We therefore set the arm so that the pitot tubes were horizontal.

Pressure measurements

Each pitot tube was connected to the positive side of its own individual differential pressure transducer (Omega type 163PC01D36). The negative sides of all 15 transducers were connected to the static probe, which was also connected to a single-sided, absolute pressure transducer (Omega type 142PC30A), making 16 transducers in all. The differential pressure transducers thus indicated the local

dynamic pressure (Q), defined as the excess of the 'total head' in the pitot tubes (H) over the static pressure (P):

$$Q = H - P. \tag{3}$$

To provide a reference source for calibrating the transducers, a separate, combined pitot-static probe (United Sensors PCC 12-KL) was mounted at the top of the support stem, with the probe 67 mm above the centre pitot tube. This was connected across a Datametrics 570D-10T-2A1-V1X Barocel differential digital manometer, whose calibration had previously been checked against a manometer. The dynamic pressure (Q) indicated by the Barocel (rather than air speed as such) was the primary reference used in setting the air speed, calibrating the pressure transducers and reducing the results. When we refer to 'air speed', we mean the equivalent air speed (V_e), defined as:

$$V_e = \sqrt{(2Q/\rho_0)}, \tag{4}$$

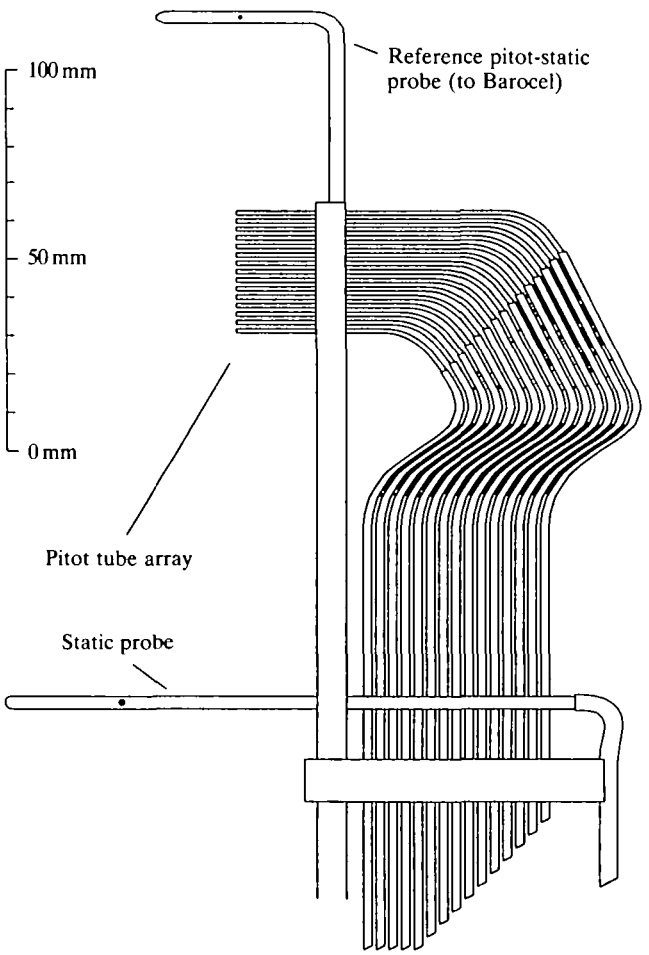

Fig. 1. Wake rake assembly.

where ρ_0 is the sea-level air density in the standard atmosphere ($1.23\,kg\,m^{-3}$) and Q is the dynamic pressure indicated by the Barocel. The true (as opposed to equivalent) air speed could be found from the dynamic pressure by using the actual air density instead of ρ_0 in equation 4. However, it was not necessary to make this distinction, as the actual air density outside the wind tunnel was very near ρ_0, increasing progressively from $1.19\,kg\,m^{-3}$ at the beginning of our experiments to $1.21\,kg\,m^{-3}$ at the end. We also neglected the effect on the air density of the static pressure difference between the air in the working section and that outside the tunnel. At the highest air speed used in calibration tests ($14\,m\,s^{-1}$), the reduction of static pressure in the working section was only about 0.3 %, as observed by our static pressure transducer.

Sampling sequence

When an observation of profile drag was initiated (by triggering the camera, as above) the flash was detected by a phototransistor mounted on the wake rake stem, which delivered a strobe pulse to an array of 16 sample-and-hold amplifiers (LF398) whose inputs were connected to the 16 pressure transducers. The sample-and-hold outputs assumed the values of the transducer outputs at the instant of the flash and held these constant while they were digitized in turn by an ADC-1 12-bit analogue to digital converter. The digitizing sequence was controlled by an Epson PX-8 laptop computer and was initiated automatically by the flash, allowing a short delay for the sample-and-hold outputs to stabilize. The computer stored the digitized readings in a data file on its built-in tape recorder. Amongst other information recorded in the data file was the time of each observation from the computer's clock, for correlation with the time imprinted on the photographs.

Before initiating a set of (usually six) observations, the free-stream dynamic pressure was set to a desired value by adjusting the tunnel speed control and observing the Barocel reading. This adjustment was made with the bird standing on the floor of the tunnel because, if the bird was standing on the perch, its proximity caused the Barocel reading to deviate from the required free-stream value. The position of the perch was constant, at the centre of the tunnel width. Observations were obtained at different spanwise positions along the wing by moving the pitot tube array and the camera in the spanwise direction.

Reduction of observations

In the original method devised by Betz (1925), the profile drag coefficient was found by sampling both the total head, H (the absolute pressure in a pitot tube), and also the static pressure, P, at a number of points across the wake. However, Pankhurst and Holder (1965), reviewing simplified variants of the original method, indicated that it is sufficient to sample the total head at a number of points, regarding the static pressure as constant. From each pitot-tube observation, the 'total head deficit' (h) is calculated, where:

$$h = (H_0 - H)/(H_0 - P_0)\,. \tag{5}$$

H_0 and P_0 are the 'free-stream' values of the total head and static pressure. Rather than sampling total head as such, the pressure transducers connected to our pitot-tube array supplied 15 measurements of the local dynamic pressure (Q), relative to a common source of static pressure. In practice, our formula for finding the total head deficit (h) for each tube was:

$$h = (Q_0 - Q)/Q_0\,, \tag{6}$$

where Q_0 is the free-stream dynamic pressure, as measured by the Barocel manometer, with the bird standing on the floor of the tunnel. This is the same as equation 5, provided the static pressure in the wake is assumed to be constant and equal to P_0, as recommended by Pankhurst and Holder (1965). The profile drag coefficient C_{Dpro} is found by summing the contributions for the 15 tubes, thus:

$$C_{\mathrm{Dpro}} = \Sigma(h\Delta y/c)\,, \tag{7}$$

where Δy is the distance between the centres of the pitot probes and c is the local wing chord, measured along the direction of the air flow, directly upstream of the probes. We measured c from the photographs, for each individual observation. Pankhurst and Holder (1965) multiply the right-hand side of equation 7 by a constant, whose maximum value is 1, but we omit this, because it appears from the nomogram provided that, under the low-speed conditions of our experiments, the value of this constant would be indistinguishable from 1.

It should be noted that this procedure gives an estimate of the *local* profile drag coefficient, referring to the chord line directly upstream of the probe. It is not a mean value for the wing as a whole and, in general, its value may be expected to vary at different spanwise positions.

Pressure transducer calibration

To calibrate the pressure transducers, the wake rake, with the reference pitot-static probe attached as shown in Fig. 1, was installed in the centre of the tunnel, and the wind speed was set by reference to the Barocel to give dynamic pressures corresponding to equivalent air speeds of 6, 8, 10, 12 and 14 $\mathrm{m\,s^{-1}}$. At each air speed, 10 observations were taken of the readings of the 15 pressure transducers. Then, a linear regression was calculated for each transducer, relating the mean digitized reading at each speed to the dynamic pressure set with the Barocel. The 15 pairs of regression coefficients were stored in a file in the computer. When analyzing data from subsequent experiments, these coefficients were retrieved and used to make the reverse transformation, from digitized reading to dynamic pressure in pascals.

Glider wing

We validated the method by measuring the drag of a pair of polystyrene model glider wings, using a drag balance, and comparing the drag coefficient with that found by the wake rake. The wing (consisting of left and right wings moulded together in a single block) was from an 'Astro-mite' model, which was described

and illustrated by Tucker and Parrott (1970). Its span was 1.12 m and area 0.167 m^2 (quite similar to those of the bird). The chord tapered from 160 mm at the root to 144 mm at the tip. The profile was biconvex, with a weakly cambered mean line, and its maximum thickness was 18 % of the chord. We supported the wing at the centre on a thin, vertical, streamlined 'sting', projecting upwards from a two-component balance measuring lift and drag. The drag of the sting, including interference drag, had previously been determined as less than 1 % of that of the wing, and was neglected. Each section of the balance, which was built by one of us (CEH), was based on a parallelogram strain gauge design given by Pope and Harper (1966). The balance was supported rigidly on a stand bolted to the floor of the tunnel, and was enclosed in a streamlined shroud. It gave independent indications of lift and drag on a digital indicator outside the tunnel. We calibrated the drag section of the balance by placing balance weights in a pan suspended from a thread, which passed over a low-friction pulley and pulled horizontally on the balance. The lift section was calibrated by standing the bird on the perch.

The experiment with the glider wing was designed to measure the wing's profile drag coefficient with the wake rake and independently with the drag balance. The balance measured the drag of the whole wing, from which the profile drag coefficient was calculated from equation 1, whereas the wake rake was positioned behind the left wing, at a point where the chord was 155 mm, and provided an estimate of the local profile drag coefficient at that point, using equation 7. To make sure that the balance measured the wing's profile drag only (not induced drag) we adjusted the angle of attack until the lift was less than the drag (usually about half the drag). If the lift coefficient were equal to the total drag coefficient (C_D), then the ratio of the induced drag coefficient (C_{Di}) to the total drag coefficient would be:

$$C_{Di}/C_D = C_D/\pi A\,, \tag{8}$$

where A is the aspect ratio (7.51 for our wing). As the highest drag coefficients we observed were around 0.03, the above criterion means that the induced drag would be no more than 0.13 % of the total drag, so that the drag observed with the balance can be considered to be the same as the profile drag.

Results and discussion

Variability of pressure measurements

The source of pressure for calibrating our array of pitot tubes and transducers was the tunnel dynamic pressure, as determined by the reference probe connected to the Barocel, at the air speeds given above. Fig. 2 shows the mean standard deviation for all the transducers, which increased with increasing speed. Extrapolating the linear regression line of Fig. 2 to zero speed gives an intercept of 0.427 Pa, which we take to be the standard deviation of the transducers themselves, in still air. We interpret the increasing standard deviation at non-zero air speeds as being due to real variations of dynamic pressure, resulting from turbulence in the air stream. From the slope of the regression line, this variable

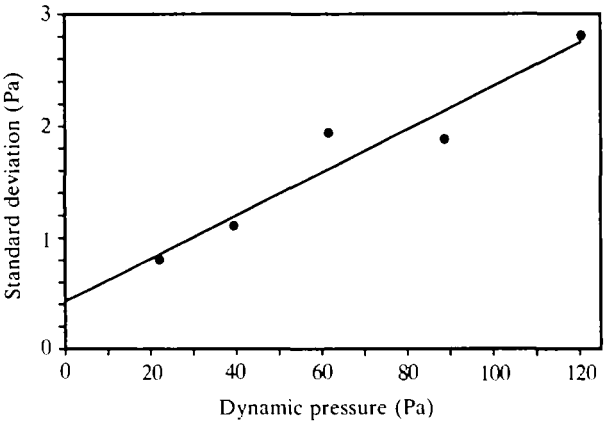

Fig. 2. Standard deviation of wake rake dynamic pressure outputs (mean for all tubes) as a function of reference free-stream dynamic pressure.

component of the standard deviation was $0.0193Q$, where Q is the dynamic pressure. However, the pressure measured by each transducer was the *difference* between the pressure in one of the dynamic probes and that in the static probe. The two probes were far enough apart to be affected independently by pressure fluctuations due to tunnel turbulence. If both are assumed to have equal standard deviations and to be randomly combined, then the observed standard deviation would be $\sqrt{2}$ times the standard deviation of either pressure source on its own. The standard deviation of the dynamic head is thus estimated to be $0.0193Q/\sqrt{2} = 0.0136Q$. Since Q varies with the square of the air speed (V), the root mean square of air speed variations would be half this, or $0.0068V$. This is somewhat below the value of 1–2 % obtained by Tucker and Parrott (1970) from hot-wire anemometer measurements in the same wind tunnel, using the same wire grid at the entrance to the working section as was installed in our experiments, but is rather high in comparison to the levels reported in wind tunnels specially designed for low turbulence, for instance 0.02 % in the Virginia Tech Stability Wind Tunnel (Marchman and Abtahi, 1985) and 0.03 % in the Bristol Low Turbulence Tunnel (Barrett, 1984).

Validation of the method using glider wing

Fig. 3 shows that the absolute values of the profile drag coefficient, estimated from the wake rake data, were close to those measured by the balance, but the standard deviations were about five times higher in the wake rake measurements than in those made with the balance. We attribute this to variations in the pressure measurements, caused by the inherent imprecision of the transducers, in combination with pressure variations due to turbulence in the wind tunnel (above).

There is a suggestion in Fig. 3 that the wake rake overestimated the profile drag coefficient when placed close to the trailing edge. As the wing profile was thick, and its trailing edge was rounded, such an effect could be caused by an area of

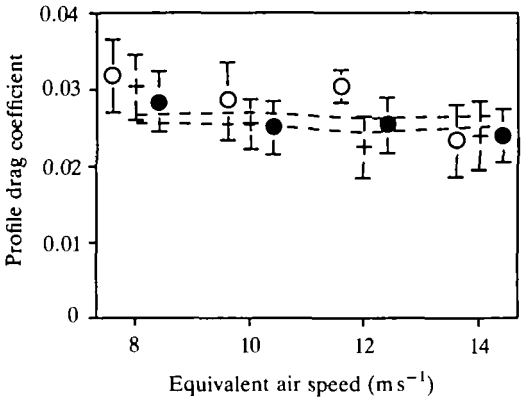

Fig. 3. Profile drag coefficient of the glider wing. Dashed lines are drag balance estimates, one standard deviation above and below the mean. The points are means of wake rake observations at distances behind the trailing edge equal to 0.25 chord (open circles), 0.5 chord (crosses) and 1 chord (filled circles). Vertical bars represent 1 standard deviation above and below the mean. Each cluster of three points was observed at one air speed, indicated by the x-position of the cross.

separated flow behind the wing. No such effect would be likely behind a bird wing, at least at low lift coefficients, because the posterior part of the profile is only one feather thick, and the trailing edge is sharply pointed. Nachtigall (1979) measured the trailing edge angle of pigeon wings as only 1.5°. We concluded from Fig. 3 that the distance of the probe behind the wing has at most a weak effect on the estimated profile drag coefficient, and we did not take account of this variable in our measurements on the bird.

We did not attempt to compare drag balance and wake rake estimates of the glider wing's profile drag over a range of angles of attack, with non-zero lift coefficients. However, Marchman and Abtahi (1985) did this at Reynolds numbers similar to ours, and reported good agreement between the two methods.

Observations on the bird

We begin by examining a particular observation in detail, before considering the range of variation in the results. In the photograph (Fig. 4) the bird can be seen holding on to the perch with his left foot, while his right foot is trailing back. His weight at the time was 7.6 N, and the upward force on the perch was 3.1 N, so that the lift developed by the wings was 10.7 N. The wing was estimated from the photograph to be nearly fully spread, with an area of 0.163 m^2. The equivalent air speed was 11 m s^{-1} ($Q = 74.4$ Pa) and the lift coefficient was 0.88. The tip of the static probe can just be seen in the photograph, and shows that the spanwise position of the observation was in zone 1 (Fig. 5A), through the proximal part of the radio-ulna, where the chord was 227 mm. The profile shape in this part of the wing was estimated by fitting a flexible plastic ruler to the upper and lower surfaces (with the bird on the bench), tracing the shapes and fitting them together. The

Fig. 4. A photograph similar to this accompanied each wake rake observation. The arrow indicates the tip of the static probe. The observations relating to this photograph are shown in Fig. 5.

resulting profile is shown at the top left of Fig. 5, set at the calculated angle of attack for the observed lift coefficient (from the computer analysis, see below). The pitot tube array is shown behind the wing, drawn to the same scale and tilted 4° to allow for the downwash. The thin lines lead from each tube to the corresponding point on the graph on the right, depicting the total head deficit (h). A value of $h = 0$ means that the dynamic pressure had its free-stream value, and the points move to the left where the air was slowed down by the wing. The profile drag coefficient is proportional to the area between the curve and the axis of $h = 0$.

The curve of Fig. 5 is typical in being generally bell-shaped, with some irregularities, and showing h declining to values near zero at both ends of the pitot tube array. Our criterion for considering the wake to be adequately centred was that there should be at least one tube with $h<0.1$, at each end of a central area with higher h. We obtained 92 observations satisfying this criterion, but missed the lift measurement on three of them, leaving 89 observations with both a lift and a drag coefficient. The mean value of h in Fig. 5 is near 0.3, which is also typical.

Bias and precision of estimate

Our approximate method (equation 6) for finding the total head deficit (h) for

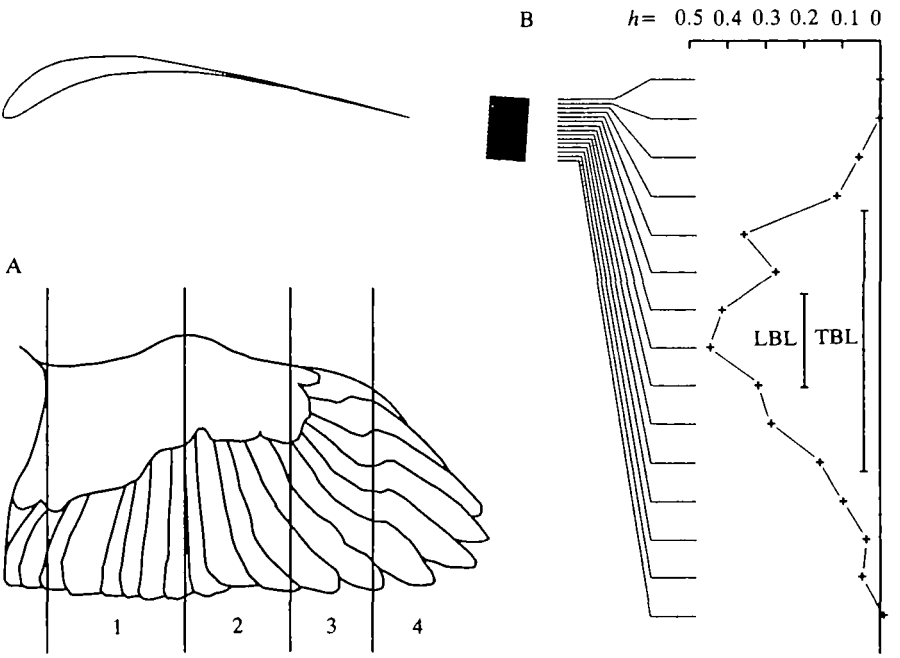

Fig. 5. (A) Spanwise zones. (B) Profile measured from the ulnar region of the hawk's wing (middle of zone 1) and wake rake observation corresponding to the photograph (Fig. 4). h, total head deficit. LBL, TBL, theoretical wake thicknesses for laminar and turbulent boundary layers (see text).

each tube of the wake rake depends on assigning a value to the 'free-stream' dynamic pressure Q_0. The presence of any object in a closed wind tunnel causes the air to accelerate around it, which means that the dynamic pressure near an object is usually slightly higher than with the tunnel empty. Some authorities measure Q_0 by adding additional pitot tubes, spaced beyond the ends of the wake rake, which is convenient in engineering applications, as it avoids having to remove a test model when setting the dynamic pressure. We found it easier to set a stable dynamic pressure with the bird standing well away from the reference pitot probe, as above, and we used this value for Q_0. If this had caused a bias, it would have been apparent in the 'tails' of the wake rake, which should show $h = 0$. In fact, the tubes at the end of the wake rake showed small positive or negative values, as in Fig. 5. This was also true in observations where the wing was too high or too low, so that several tubes were clear of the wake, indicating that there was no appreciable bias from this cause.

The variation of dynamic pressure due to tunnel turbulence (above) corresponds to a standard deviation of 0.0193 for h, or about 6 % of the mean value of h. Most observations of profile drag coefficient were obtained by adding together eight or fewer observations of h (see below). If the errors were independent for the different pitot tubes, the resultant error would be $\sqrt{(8\times0.06^2)}$ or about 17 %.

However, this may be pessimistic, as the tubes were close enough together that pressure variations would most likely be correlated between tubes.

Air speed and Reynolds number

Our observations on the bird were confined to equivalent air speeds in the range 10–13 $m\,s^{-1}$. In calculating the Reynolds number (equation 2), we measured the chord from the photographs and assumed that the kinematic viscosity of the air was constant at $1.45\times10^{-5}\,m^2\,s^{-1}$. Apart from one observation with $Re = 83\,000$ (very near the wing tip, where the chord was small), our Reynolds numbers were in the comparatively narrow range 143 000–194 000, which was insufficient to observe any systematic change in the profile drag coefficient, as a function of Reynolds number.

Spanwise zones

As shown in Fig. 5A, we divided the wing into four spanwise zones, named 1–4. Zone 1 is the propatagial zone, where the leading edge is drooped by the patagial tendon. Zone 2 is the zone in which the bird might be able to modify the flow over the wing by raising the alula. Zone 3 is the zone in which the wing is only one feather thick throughout the whole chord, and zone 4 is the zone of emarginated primaries and slots. The mean profile drag coefficients for the different zones were only slightly different but the standard deviation was higher in zone 2 than in zones 1 or 3 (Fig. 6). Zone 4 (in which we only obtained three observations) is of little interest, because the transverse components of flow, caused by wing-tip vortices, would invalidate the wake rake measurement. All zones showed higher standard deviations than were seen in the glider wing. This is partly because the glider wing was tested at a constant lift coefficient (near zero), whereas the bird's lift coefficients ranged from 0.51 to 1.08. However, the standard deviation for zone 2

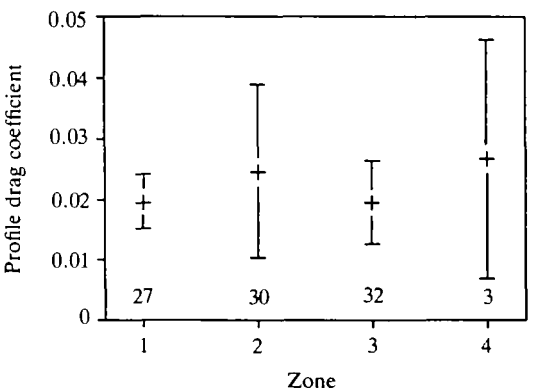

Fig. 6. Means and standard deviations of profile drag coefficients estimated from wake rake observations, from the different spanwise zones defined in Fig. 5. The numbers of observations in each zone are shown at the bottom.

(three times that of the glider wing) was higher than those for zones 1 and 3 (1.2 and 1.7 times that of the glider wing, respectively).

Fig. 6 suggests that the variation was caused, at least in part, by real variations of profile drag, due to the bird adjusting its wings, as the standard deviation in the least variable zone (1) was about 23 % of the mean, or about 1.4 times the amount that could be attributed to turbulence in the wind tunnel (above). The high variability in zone 2 might suggest that the bird was continually making small adjustments, both positive and negative, to its profile drag, and that this action was mediated by variations of shape in the carpo-metacarpal region of the wing, more so than in the more proximal or distal regions. The highest lift coefficients in our sample would appear to be rather low for the alula to be raised, but we were not able to investigate this, as the alula was not visible in our photographs.

Polar plot

In Fig. 7, the 89 observations of lift coefficient have been plotted against the profile drag coefficient, in the manner of the classical polar plot. Tucker and Heine (1990) presented a similar plot for the same bird, gliding in the same wind tunnel, but their estimates of profile drag coefficient were obtained by subtraction (see above) and referred to the wing as a whole, whereas the wake rake method effectively 'dissects out' a chord line and measures the local profile drag coefficient at that location. Tucker and Heine discussed their results in terms of Tucker's (1987) concept of a 'polar area', rather than a polar curve. The dashed curve (*A*) was plotted from their equation 22, representing their best estimate of the minimum profile drag coefficient for the whole wing, as a function of lift

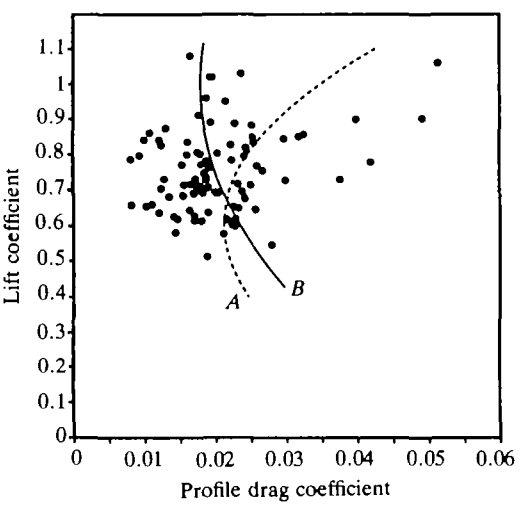

Fig. 7. Wake rake observations in the format of a polar diagram. Curve *A* is the left (minimum drag) boundary of Tucker and Heine's (1990) 'polar area'. Curve *B* is the polar curve calculated by the Airfoil-ii computer program, for the profile shape shown in Fig. 5, at $Re = 175\,000$.

coefficient. In the polar area concept, points can fall to the right of this line, if the bird creates additional drag, but not to the left. Evidently, a majority of our points fall to the left of the *minimum* drag coefficient shown by curve *A* (about 0.02). This could be because our estimates refer mostly to the broader parts of the wing, where the Reynolds number is highest, so that the local profile drag coefficients which we observed could have been lower than the average for the whole wing, as observed by Tucker and Heine. Alternatively, if Tucker and Heine had overestimated the total drag, or underestimated the induced and/or parasite drag, this would have led to an overestimate of the profile drag. As all three of these estimates are not without their difficulties, an error from this source is possible.

The scatter of our observations is rather wide in relation to the estimated precision of the drag coefficient estimates (17 % or less, see above). The points in Fig. 7 do not seem to be distributed along a well-defined curve, as usually occurs in wind tunnel tests on rigid models. This raises the interesting possibility that the bird may have been making active movements of its wings, too small to be readily apparent to an observer, which can either increase *or decrease* the local profile drag coefficient of a specific chord line. To bring about a decrease in the local drag coefficient, the bird would have to move its wing in a way that causes the boundary layer to accelerate. We actually observed this on a gross scale, on one occasion when the operator triggered the camera just as the bird let go of the perch and flapped its wings. It so happened that the wake (or part of it) was intercepted by the wake rake. All 15 tubes showed negative values of h, and the calculated profile drag coefficient was -0.0237. The flapping action caused the wake to be accelerated instead of being retarded, meaning that the wing was producing thrust instead of drag. Fig. 6 suggests that active control movements, which modify the local profile drag coefficient, are centred on the carpo-metacarpal region of the wing.

Computer analysis of profile

The profile shape shown in Fig. 5 was digitized and entered as input to a commercially available program, Airfoil-ii by Airware. The operation of this program is described by Eppler and Somers (1980). It was primarily intended for designing aerofoil shapes with specified properties, but can also be used to predict the properties of an existing profile. According to the manual, it has been successfully used at Reynolds numbers as low as 20 000. Analyzing the profile of Fig. 5 at $Re = 175\,000$, it produced the polar plot shown as curve *B* in Fig. 7. It also predicted that the maximum lift coefficient at this Reynolds number would be 1.40, which is somewhat less than the value of 1.6 reported for the same bird by Tucker and Heine (1990). The predictions indicated that the maximum lift coefficient would be quite sensitive to Reynolds number, increasing from 1.36 at $Re = 150\,000$ to 1.44 at $Re = 200\,000$.

The profile shown in Fig. 5 may be too strongly cambered since, as Nachtigall (1979) pointed out, the action of the lift flattens the camber somewhat when the bird is in flight. Bird wing profiles generally are very thin, being only one feather

thick in the posterior and distal parts, and their mean lines are also more strongly cambered than typical aerofoils for model aircraft, at least when the wing is fully stretched out. Pressnell (1977) illustrates a wide selection of profile shapes, recommended for use in model aircraft at bird-like Reynolds numbers, none of which is as thin or as strongly cambered as our hawk's profile in Fig. 5. This profile was 6.7 % thick and quite similar to the thin, cambered plate (Göttingen 417a) for which Schmitz (1960) presented measured performance curves at various Reynolds numbers. His polar curve for $Re = 168\,000$ (within the range of our observations) shows a minimum profile drag coefficient of 0.020 at a lift coefficient, C_L, of 0.80. If this curve were drawn on Fig. 7, it too would pass through our data points.

If our speculation is correct, that the bird can momentarily either increase or decrease the local drag coefficient of a particular part of the wing, then one could interpret curve *B* as being the polar plot of the dead wing. Active movements of the live wing would cause particular points to deviate either to the left or to the right of the curve. The few points scattered far to the right could be due to separation of the boundary layer, which also might be actively induced by the bird for control purposes.

Thickness of the wake and the boundary layer

Fig. 5B gives a direct visual impression of the thickness of the wake, which represents the boundary layers on the upper and lower surfaces of the wing, plus any dead space between them due to separated flow. Wakes and boundary layers do not have sharp edges, so we defined the 'edge' by the arbitrary criterion that $h>0.1$ within the wake. Fig. 8 shows the distribution of wake thickness, as measured by the number of 'active' tubes, with $h>0.1$. The graph of Fig. 5, with eight active tubes, is to the right of the peak, most observations having 5–7 active tubes. One observation had only two active tubes, and a few had up to 11.

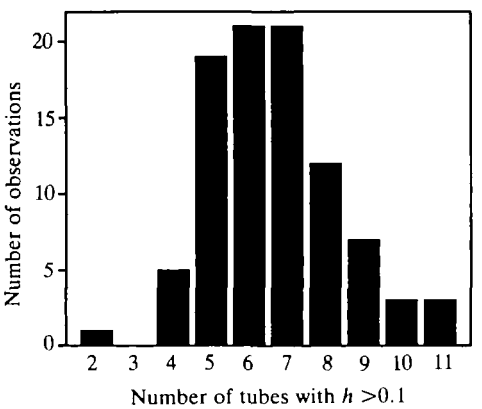

Fig. 8. Distribution of wake thickness, as gauged by the number of pitot tubes showing $h>0.1$.

Boundary layers are normally thicker if turbulent than if laminar. According to Ashley and Landahl (1965), the thickness (δ) of a laminar boundary layer at the trailing edge of a flat plate may be estimated as:

$$\delta = 5c/(Re)^{1/2}, \tag{9}$$

whereas that of a turbulent boundary layer is:

$$\delta = 0.37c/(Re)^{1/5}, \tag{10}$$

where c is the chord. If the boundary layers were attached on both surfaces of the wing, with no appreciable dead space between them, then our 'tube count' would estimate their combined thickness, corresponding to 2δ. For the observation illustrated in Fig. 5, we used $c = 227$ mm and $Re = 172\,000$ to get estimates of 2δ from equations 9 and 10. The results are shown as vertical bars in Fig. 5. The bar marked TBL (for turbulent boundary layer) is equivalent to 6.9 tubes, whereas the bar marked LBL (laminar boundary layer) extends over 2.5 tubes. Only one of the 92 observations in Fig. 8 (the one with two active tubes) could be interpreted as an attached laminar boundary layer. The bulk of the observations, with 5–8 active tubes, are consistent with an attached boundary layer that is mostly or entirely turbulent or with a laminar one that is partially separated. The few observations with 9–11 active tubes are most easily explained as being due to separated flow, possibly induced by the bird as an active means of increasing drag for control purposes.

In conclusion, our observations of profile drag coefficient are consistent with those which Tucker and Heine (1990) made by the subtractive method on the same bird, although it has to be remembered that our observations are estimates of the profile drag coefficient of a two-dimensional profile, at a particular point on the wing, whereas those of Tucker and Heine are average values for the wing as a whole. The scatter in our observations is greater than could be accounted for by the imprecision of measurement (estimated to be no more than 17 %) and suggests that the bird can actively vary the local profile drag by movements of the wing, especially in the carpo-metacarpal area. Comparison with Tucker and Heine's estimates suggests that these variations can be negative as well as positive, that is, that the bird is capable of momentarily accelerating the boundary layer by active movements of the wing. If the basis of these control movements could be identified, it might have aeronautical applications.

Studies such as those of Schmitz (1960) and Marchman and Abtahi (1985), on wing models at bird-like Reynolds numbers, have drawn attention to the fact that the behaviour of the boundary layer can be strongly affected by turbulence in the air stream, meaning that the lift and drag properties of a given wing, observed in a wind tunnel with turbulence, may differ significantly from the properties of the same wing in free flight. The level of turbulence in the Duke University wind tunnel is high enough to raise doubts about the validity of the results, when used to calculate the performance of free-flying birds, and there is no reason to believe that other wind tunnels that have been used for bird flight experiments are

appreciably better in this respect. These doubts apply to many published results in addition to the present observations and can only be resolved by constructing a low-turbulence wind tunnel, especially for bird flight experiments.

We are deeply indebted to Dr Vance Tucker for providing us with facilities to use the bird and the wind tunnel at Duke University and to him and Dr Steven Vogel for lending us numerous essential items of equipment and helping us throughout the project. We also thank Dr Tucker for his detailed comments on the first draft of the manuscript, which enabled us to rectify a number of errors and omissions. Funding for the project was provided under Cooperative Agreement no. 14-16-0009-86-965 between Sea and Sky Foundation and the US Fish and Wildlife Service. Mention of product names does not imply endorsement by the U.S. government.

References

ANDERSON, J. D. (1984). *Fundamentals of Aerodynamics.* New York: McGraw Hill.

ASHLEY, H. AND LANDAHL, M. (1965). *Aerodynamics of Wings and Bodies.* Reading, MA: Addison-Wesley. (Dover edition 1985).

BARRETT, R. V. (1984). Design and performance of a new low turbulence wind tunnel at Bristol University. *Aeronaut. J. R. aeronaut. Soc.* 86–90.

BETZ, A. (1925). A method for the direct determination of wing section drag. *NACA Technical Memorandum no. 337.*

EPPLER, R. AND SOMERS, D. M. (1980). A computer program for the design and analysis of low-speed airfoils. *NASA TM 80210.* 140pp.

MARCHMAN, J. F. AND ABTAHI, A. A. (1985). Aerodynamics of an aspect ratio 8 wing at low Reynolds numbers. *J. Aircraft* **22**, 628–634.

NACHTIGALL, W. (1979). Der Taubenflügel in Gleitflugstellung: Geometrische Kenngrössen der Flügelprofile und Luftkrafterzeugung. *J. f. Ornithologie* **120**, 30–40.

PANKHURST, R. C. AND HOLDER, D. W. (1965). *Wind-tunnel Technique.* 2nd edn. London: Pitman.

PENNYCUICK, C. J. (1968). A wind-tunnel study of gliding flight in the pigeon *Columba livia. J. exp. Biol.* **49**, 527–555.

PENNYCUICK, C. J. (1989). *Bird Flight Performance: A Practical Calculation Manual.* Oxford: Oxford University Press.

PENNYCUICK, C. J., OBRECHT, O. O. AND FULLER, M. J. (1988). Empirical estimates of body drag of large waterfowl and raptors. *J. exp. Biol.* **135**, 253–264.

POPE, A. AND HARPER, J. (1966). *Low-speed Wind Tunnel Testing.* New York: Wiley.

PRESSNELL, M. (1977). *Aerofoils for Aeromodellers.* London: Pitman.

SCHMITZ, F. W. (1960). *Aerodynamik des Flugmodells* (4th edn). Duisberg: Lange.

SPEDDING, G. R. (1987). The wake of a kestrel (*Falco tinnunculus*) in gliding flight. *J. exp. Biol.* **127**, 45–57.

TUCKER, V. A. (1987). Gliding birds: the effect of variable wing span. *J. exp. Biol.* **133**, 33–58.

TUCKER, V. A. (1990*a*). Body drag, feather drag and interference drag of the mounting strut in a peregrine falcon, *Falco peregrinus. J. exp. Biol.* **149**, 449–468.

TUCKER, V. A. (1990*b*). Measuring aerodynamic interference drag between a bird body and the mounting strut of a drag balance. *J. exp. Biol.* **154**, 439–461.

TUCKER, V. A. AND HEINE, C. (1990). Aerodynamics of gliding flight in a Harris' hawk, *Parabuteo unicinctus. J. exp. Biol.* **149**, 469–489.

TUCKER, V. A. AND PARROTT, G. C. (1970). Aerodynamics of gliding flight in a falcon and other birds. *J. exp. Biol.* **52**, 345–367.

VOGEL, S. (1981). *Life in Moving Fluids: The Physical Biology of Flow.* Princeton: Princeton University Press.